Author Manuscript

Author Manuscript

Author Manuscript

Author Manuscript

HHS Public Access

Author manuscript

Neuroimage. Author manuscript; available in PMC 2023 July 15.

Published in final edited form as:

Neuroimage. 2023 July 15; 275: 120167. doi:10.1016/j.neuroimage.2023.120167.

Associations between age, sex, APOE genotype, and regional vascular physiology in typically aging adults

Nikou L. Damestani[a,b,*], **John Jacoby**[a], **Shrikanth M. Yadav**[a], **Allison E. Lovely**[a], **Aurea Michael**[a], **Melissa Terpstra**[c], **Marziye Eshghi**[d], **Barnaly Rashid**[a,e], **Carlos Cruchaga**[f,g,h], **David H. Salat**[a,b,i], **Meher R. Juttukonda**[a,b,*]

[a]Athinoula A. Martinos Center for Biomedical Imaging, Department of Radiology, Massachusetts General Hospital, Charlestown, MA, USA

[b]Department of Radiology, Harvard Medical School, Boston, MA, USA

[c]Center for Magnetic Resonance Research, Department of Radiology, University of Minnesota, Minneapolis, MN, USA

[d]MGH Institute of Health Professions, Boston, MA, USA

[e]Department of Neurology, Harvard Medical School, Boston, MA, USA

[f]Department of Psychiatry, Washington University School of Medicine, St. Louis, MO, USA

[g]NeuroGenomics and Informatics Center, Washington University School of Medicine, St. Louis, MO, USA

[h]Hope Center for Neurologic Diseases, Washington University in St. Louis, St. Louis, MO, USA

[i]Neuroimaging Research for Veterans Center, VA Boston Healthcare System, Boston MA, USA

Abstract

Altered blood flow in the human brain is characteristic of typical aging. However, numerous factors contribute to inter-individual variation in patterns of blood flow throughout the lifespan. To better understand the mechanisms behind such variation, we studied how sex and *APOE* genotype, a primary genetic risk factor for Alzheimer's disease (AD), influence associations between age and brain perfusion measures. We conducted a cross-sectional study of 562 participants from the Human Connectome Project - Aging (36 to >90 years of age). We found widespread associations between age and vascular parameters, where increasing age was associated with regional decreases in cerebral blood flow (CBF) and increases in arterial transit time (ATT). When grouped by sex and *APOE* genotype, interactions between group and age demonstrated that females had relatively

This is an open access article under the CC BY-NC-ND license (http://creativecommons.org/licenses/by-nc-nd/4.0/)

*Corresponding author. 149 Thirteenth Street, Suite 2301, Charlestown, MA, 02129, USA. ndamestani@mgh.harvard.edu (N.L. Damestani), mjuttukonda@mgh.harvard.edu (M.R. Juttukonda).

Declaration of Competing Interest

None.

Financial Disclosures

All authors declare that they have no competing interests in relation to this manuscript.

Supplementary materials

Supplementary material associated with this article can be found, in the online version, at doi:10.1016/j.neuroimage.2023.120167.

Author Manuscript Author Manuscript Author Manuscript Author Manuscript

greater CBF and lower ATT compared to males. Females carrying the *APOE ε*4 allele showed the strongest association between CBF decline and ATT incline with age. This demonstrates that sex and genetic risk for AD modulate age-associated patterns of cerebral perfusion measures.

Keywords

Perfusion MRI; Aging; Arterial spin labeling; Healthy aging; *APOE*; Sex differences; Cerebral blood flow; Arterial transit time

1. Introduction

Understanding the characteristics of typical brain aging is fundamental for identifying atypical age-related changes and for distinguishing early biomarkers of pathology associated with neurodegeneration. Previous work has demonstrated that brain perfusion decreases with advancing age (Chen et al., 2013, 2011) and has suggested that physiological properties, including tissue hypoperfusion, precede detectable alterations in brain structure or cognition (Mokhber et al., 2021; Li et al., 2021). One of the main roles of cerebral perfusion is supplying the nutrients necessary for cerebral metabolism and neuronal function, and reduced perfusion is associated with brain tissue damage and neural dysfunction (Love and Miners, 2016). Therefore, characterizing cerebral hemodynamic physiology is critical for improving our understanding of the aging process.

Arterial spin labeling (ASL) magnetic resonance imaging (MRI) allows for noninvasive quantitative measurement of cerebral hemodynamics by using arterial blood water as an endogenous tracer (Williams et al., 1992). Arterial blood water in the cervical arteries is ‘labeled’ using a series of radiofrequency pulses. This labeling period is followed by a post-labeling delay to allow the labeled blood to reach and perfuse brain tissue. Images acquired including this ‘label’ are subtracted from ‘control’ images acquired with no labeling, and this difference is used to quantify cerebral blood flow (CBF), which represents the perfusion rate of blood from cerebral capillaries into brain tissue.

Declining CBF in global gray matter with advancing age has been widely observed with ASL (Alisch et al., 2021; Juttukonda et al., 2021; Chen et al., 2013, 2011). However, conventional ASL imaging is typically acquired with one post-labeling delay, capturing the labeled blood that arrives to and perfuses brain tissue by this one time point. The temporal delay between labeling of the blood and its arrival to brain tissue is known as the arterial transit time (ATT), and ATT variation has been demonstrated in aging and in disease associated with changes in cerebral vasculature. By acquiring multiple post-labeling delays, known as ‘multi-delay’ ASL (Wang et al., 2013; OSIPI Task Force 4.1, 2022), it is possible to capture the variation in ATT between and within individuals. This provides additional information regarding vessel tortuosity and structure, which particularly benefits studies of aging (Mutsaerts et al., 2017). However, studies of ATT in aging have been limited as early multi-delay ASL methods produced elongated scan duration.

Accelerated MR imaging methods alongside multi-delay ASL have made it possible to acquire high-resolution data in a relatively short period (~5.5 min), as implemented as part

Author Manuscript Author Manuscript Author Manuscript Author Manuscript

of the imaging protocol for the Human Connectome Project Aging (HCP-A) study (Harms et al., 2018). A recent study presented a novel modeling approach tailored to obtain reliable ATT measures in older adults using multi-delay ASL data from HCP-A (Juttukonda et al., 2021). Using this approach for a subset of the HCP-A cohort, ATT increases and CBF decreases were identified globally in gray matter with advancing age.

Despite these advances, it remains to be determined whether specific regions of the cerebral cortex exhibit greater microvascular perfusion deficits during aging and whether some regions are hyperperfused (Wang et al., 2021; Chen et al., 2011; Parkes et al., 2004). Regional perfusion differences at a given age might also differ by biological sex (Parkes et al., 2004; Juttukonda et al., 2021; Alisch et al., 2021) and by the presence of an $\varepsilon 4$ allele of the apolipoprotein-E (*APOE*) gene (Wang et al., 2021; Wierenga et al., 2013), which is the most significant and common genetic risk factor for developing late-onset Alzheimer's disease (AD) (Rabinovici, 2019). Furthermore, the impact of the $\varepsilon 4$ allele may depend on sex, with studies suggesting that *APOE* $\varepsilon 4$ produces a greater AD risk in females (Altmann et al., 2014).

Given this range of contributing factors, large cohort studies with advanced perfusion imaging are crucial to understanding the effect of the aging process on hemodynamic function. HCP-A is likely the largest cohort to-date with multi-delay ASL data and containing a rich multi-modal dataset that captures a range of information on the aging process (Bookheimer et al., 2019; Harms et al., 2018). In this study, we extended previous approaches (Juttukonda et al., 2021) to a larger sample of the HCP-A cohort to investigate CBF and ATT variation with age. We stratified by both sex and *APOE* genotype with the goal of better understanding how these crucial factors may impact cerebral hemodynamics with healthy aging in distinct regions of the cortex and subcortex.

2. Materials and methods

2.1. Data and code availability statement

The Human Connectome Project datasets and standard processing scripts are publicly available, with access details available at https://www.humanconnectome.org/. Analyses were performed using publicly available software tools.

2.2. Study participants

Over 1200 healthy adults have been recruited for the Human Connectome Project Aging (HCP-A) study, between the age of 36 and 90+. Institutional Review Board approval was obtained, and all participants provided written, informed consent. The details of inclusion and exclusion criteria were described previously (Bookheimer et al., 2019), and all participants exhibited typical health for their age. Typical health, as discussed by Bookheimer et al. (2019), does not exclude those with prevalent health conditions (e.g., hypertension), but does exclude those with suspected Alzheimer's disease or symptomatic stroke. No participants were excluded based on medication use. This ensures the HCP-A sample is representative of the aging process.

Author Manuscript Author Manuscript Author Manuscript Author Manuscript

Four acquisition sites used matched MRI scanning protocols. Participants from the public release of the HCP-A cohort were included if ASL data were available. 677 participants met our criterion of having undergone multi-delay ASL acquisition. For the analyses of *APOE* genotype, our criteria for inclusion were participants with genotypes 1) homozygous *APOE*-ε3 (ε3/ε3), 2) either heterozygous (ε2/ε4, ε3/ε4) or homozygous (ε4/ε4) *APOE*-ε4 individuals, 3) either heterozygous (ε2/ε3) or homozygous *APOE*-ε2 (ε2/ε2) individuals within the cohort. 562 participants met this criterion. A flowchart of the exclusion process is shown in Fig. 1.

The demographics of interest and the stratification of the groups for this study are summarized in Table 1. The following measures of cardiometabolic health were also acquired in HCP-A (Bookheimer et al., 2018), which can be used to account for potential related changes in perfusion measures: body mass index (BMI), cholesterol, systolic blood pressure, diastolic blood pressure, insulin, hemoglobin A1C, LDL, triglyceride, and C-reactive Protein. These measures were adjusted to account for medication use as described by Robertson et al. (2017).

For the age association plots and accompanying analyses (Section 2.7.1 and 2.7.2), participants over the age of 90 were removed due to privacy concerns.

2.3. APOE genotyping

APOE genotyping was determined as previously described (Cruchaga et al., 2010). In brief, *APOE* ε2, ε3 and ε4 isoforms were determined by genotyping rs 7412 and rs429358 using Tagman genotyping technology.

2.4. Data acquisition

Details regarding imaging acquisition have been reported previously (Juttukonda et al., 2021; Harms et al., 2018), and important parameters related to the acquisitions utilized are briefly presented here. Two-dimensional pseudo-continuous ASL data were acquired without background field suppression to avoid signal loss. The acquisition parameters included: labeling duration = 1500 ms, five post-labeling delays (PLD) of length = 200 ms (control/label pairs = 6), 700 ms (pairs = 6), 1200 ms (pairs = 6), 1700 ms (pairs = 10), and 2200 ms (pairs = 15). No vascular crushing was applied, therefore only macrovascular metrics were investigated. The range of PLDs employed are sufficient to account for age-related transit delays, as validated by Dai et al. (2017). Additionally, the pCASL acquisition included multi-band 2D gradient-echo echo-planar imaging (EPI) readout with TR = 3580 ms, TE = 19 ms, partial Fourier = 6/8, simultaneous multislice (SMS) acceleration factor = 6, total slices = 60, spatial resolution = 2.5 × 2.5 × 2.5 mm^3, total acquisition time = 5.5 min. Two equilibrium magnetization (M_0) images were acquired at the end of the scan for calibration purposes.

To correct field inhomogeneity-related distortions, two spin echo EPI scans with opposite phase encoding directions were acquired, with TR = 8000 ms, TE = 40 ms, spatial resolution = 2.5 × 2.5 × 2.5 mm^3. A T_1-weighted image was acquired using multi-echo MPRAGE,

Author Manuscript Author Manuscript Author Manuscript Author Manuscript

with TR = 2500 ms, TI = 1000 ms, TE = 1.8, 3.6, 5.4, 7.2 ms, and spatial resolution = 0.8 × 0.8 × 0.8 mm^3 .

2.5. Physiological image processing

Susceptibility distortions were corrected for by applying 'TopUp' (Andersson et al., 2003; Smith et al., 2004) with the opposite polarity spin echo EPI scans. Multi-band accelerated readout can produce artifacts such as signal overlap between simultaneously excited slices (Xu et al., 2013). This was corrected for by interpolating the last slice of each band with the slices on either side. Motion correction was performed using AFNI '3dvolreg' (Cox, 1996). Control and label ASL data were pair-wise subtracted and averaged for each PLD. The averaged images were then calibrated for CBF quantification to the second M_0 image, in line with Juttukonda et al. (2021).

2.5.1. Arterial transit time—A cross-correlation-based approach was used to calculate ATT values based on a two-stage approach described previously (Juttukonda et al., 2021). First, each voxel was assigned a "shift index" based on the temporal shift at which the acquired signal time course in that voxel exhibited the maximum correlation with the theoretical time course, which provided a coarse estimate of ATT at the temporal resolution of the ASL acquisition (i.e., 500 ms). Next, a second cross-correlation analysis was used to provide a more fine-tuned temporal resolution of 100 ms by narrowing the search window to arrival times pre-determined by the shift index from the previous step. This two-stage approach was utilized to limit the potential for noise to result in a highly erroneous result.

2.5.2. Cerebral blood flow—An established two-compartment model at each PLD was used to extract CBF values as previously described (Wang et al., 2002; Juttukonda et al., 2021) (Eq. (1))

$$CBF_i = \frac{6000 \cdot \lambda \cdot \Delta M_i \cdot \exp\left(\frac{\delta}{T_{1,a}}\right)}{2 \cdot \alpha \cdot M_0 \cdot T_{1,a} \cdot \left[\exp\left(-\frac{\max(PLD_i - \delta, 0)}{T_{1,t}}\right) - \exp\left(-\frac{\max(\tau + PLD_i - \delta, 0)}{T_{1,t}}\right)\right]} \quad (1)$$

where the blood-brain partition coefficient $\lambda = 0.9g/\mathrm{ml}$, ΔM_{PLD} is the ASL difference signal in each voxel, $\alpha = 0.85$ is the labeling efficiency, M_0 is the equilibrium magnetization in each voxel, $T_{1,a}$ is the longitudinal relaxation of arterial blood, $T_{1,t}$ is the longitudinal relaxation time of tissue, PLD_i is the post-labeling delay for the given PLD (i), $\tau = 1.5s$ is the labeling duration, and δ is the ATT in each voxel.

$T_{1,a}$ was calculated as indicated in Eq. (2) (Lu et al., 2004)

$$T_{1,a} = \frac{1}{0.52 \cdot Hct + 0.38} \quad (2)$$

where Hct is the hematocrit. The Hct value was derived from the median of the appropriate age and sex values for each participant as determined by Mahlknecht and Kaiser (2010).

Author Manuscript Author Manuscript Author Manuscript Author Manuscript

CBF maps were derived using a least-squares fitting of Eq. (1) using data from all PLDs along with ATT values computed as described in Section 2.2.

2.6. Structural image processing

Freesurfer was used to segment the cortical regions of interest and reconstruct the cortical surfaces from the T_1-weighted image (Dale et al., 1999; Fischl et al., 1999). Images were inspected for artifacts and excessive white matter lesion volume for quality control purposes.

2.7. Surface-based group analysis

M_0 images were registered to the T_1-weighted image using boundary-based registration (Greve and Fischl, 2009). Partial volume effects were then accounted for using PET Surfer (Greve et al., 2016). After applying partial volume correction, the ATT and CBF volumes were converted to surfaces and registered to Freesurfer's 'fsaverage' surface atlas. A smoothing kernel of 15 mm FWHM was applied. The mean of each of Freesurfer's 34 gray matter cortical segmentations (Desikan et al., 2006) within each hemisphere were calculated using Freesurfer's 'mri_segstats'. Volume-wise analysis was also performed using 7 subcortical structures, according to the automated 'aseg' segmentation in Freesurfer (Fischl et al., 2002).

Cardiovascular risk was accounted for using a composite average z-score computed from the medication-adjusted measures (Section 2.2) after testing for normality using Q-Q plots and Shapiro-Wilks test. The Framingham Risk Score was not used due to the interest of the study in age and sex effects.

Participants were stratified by sex and *APOE* genotype and general linear model analyses of gray matter ATT and CBF were performed on the surfaces. The contrasts in Table 2 were used, with significance threshold established at $p < 0.05$ after permutation testing with 1000 permutations, including a cluster-forming threshold of $p = 0.001$ and cluster-wise multiple comparisons correction using threshold-free cluster enhancement in Freesurfer. As discussed by Greve and Fischl (2018), non-parametric permutation testing appropriately controls for false positive rates across hemispheres. Each hemisphere was analyzed separately given previous findings of asymmetry between groups according to sex and *APOE* genotype (Wierenga et al., 2013).

For the *APOE* genotype analyses, the output vertex-wise 'gamma' maps from Freesurfer were used to compute the effect size maps (i.e., Cohen's D) to acknowledge the differences in sample size prevalent between *APOE* genotype groups.

2.7.1. Interaction analysis—To understand the association of age, sex and *APOE* on perfusion measures, two Gaussian general linear models were tested for significance. Both included, age, sex, cardiovascular risk and *APOE* genotype as independent regressors, however one model (**Model 1**) included the interaction of sex and *APOE* genotype and the other (**Model 2**) included the interaction of sex, age and *APOE* genotype. These models were computed for each of the 34 cortical regions and 7 subcortical regions in each hemisphere, and confidence intervals were computed for each term. Statistical significance

Author Manuscript Author Manuscript Author Manuscript Author Manuscript

was established for the interaction term at $p < 0.05$ after false discovery rate (FDR) correction across the number of regions tested (p_{FDR}).

2.7.2. Slope of association analysis—The slope of association (i.e., line of best fit) was computed for each of the 34 cortical and 7 subcortical regions between the CBF or ATT measures and age. To understand the general association of perfusion measures with age, the average of all slopes and the standard deviation were computed to create a global measure of the rate of CBF and ATT change across brain regions. This was repeated after stratifying for sex and *APOE* genotype, respectively. A non-linear slope of association plot was produced for visualization to validate the relationship linearity.

The linear slopes of association were statistically compared according to group, both in terms of the mean difference between slopes (i.e., whether there is on average higher/lower CBF or ATT between groups) and the gradient of the slopes (i.e., whether CBF or ATT increases/decreases at a faster rate between groups) for each cortical and subcortical region. When comparing between sex (e.g., male vs female) or between genotype (e.g., $\varepsilon 2$ individuals vs $\varepsilon 4$ individuals), the interaction of age and the variable of interest was modeled and compared using the least squares means package version 2.30.0 in R (Lenth, 2016). The resultant p-values were then corrected for multiple comparisons using FDR correction across regions.

The gradients of the linear slopes of association between CBF or ATT with age after stratifying into both *APOE* genotype and sex (e.g., female $\varepsilon 4$ vs male $\varepsilon 4$) were extracted for each region. The groups were then compared using a simple Welch's two sample T-test with a significance threshold of $p < 0.05$.

3. Results

3.1. Associations between age and perfusion measures

We first studied the association of age with CBF and ATT measures across the entire cohort. When comparing linear slopes of association, we found that ATT was longer at older age (0.0768 ± 0.0127s per decade) and CBF was lower at older age (−3.05 ± 1.06 ml/100g/min per decade) on average across cortical gray matter and hemispheres. These patterns were consistent on average across the subcortical regions (CBF: −1.05 ± 0.895 ml/100g/min per decade; ATT: 0.0648 ± 0.0152s per decade). Fig. 2 includes the plots of the change in CBF and ATT with age on average across cortical and subcortical regions. Supplementary Material A demonstrates the impact of controlling for global gray matter CBF and ATT.

However, as demonstrated in Fig. 3, the spatial distribution of the association with age differs between ATT and CBF, with the largest effects seen for CBF in the superior frontal cortex and for ATT in the right caudal middle frontal, right inferior parietal and left superior temporal cortices. More widespread age effects are seen in ATT than in CBF, with the most overlap between the two effects being in the frontal and parietal cortices.

Author Manuscript Author Manuscript Author Manuscript Author Manuscript

3.2. The effect of sex on perfusion measures

Fig. 4 details the surface analysis of ATT and CBF for the contrast between males and females after controlling for the effect of age. Significant ($p_{TFCE} < 0.05$) differences between sex in both ATT and CBF were widespread across the cortex, with females demonstrating elevated CBF in parietal and frontal cortices and males demonstrating longer ATT in the temporal and inferior parietal regions.

Fig. 5 shows the average cortical and subcortical non-linear slope of association between CBF and ATT with age, distinguished by sex. Across all 34 cortical regions, within each hemisphere, statistically significant ($p_{FDR} < 0.05$) differences were found in the mean linear CBF and ATT slopes, supporting the previous finding. In the subcortex, significantly higher ($p_{FDR} < 0.05$) mean CBF for females was found bilaterally in the caudate, hippocampus, putamen, and thalamus whereas significantly longer ($p_{FDR} < 0.05$) mean ATT in males was found in all 7 subcortical regions.

No statistically significant differences ($p > 0.05$) were found between sex for the CBF and ATT linear slopes of association with age for any subcortical or cortical region, suggesting that CBF decreased with age and ATT increased with age at similar rates for both males and females.

3.3. The effect of APOE genotype on perfusion measures

When comparing *APOE* genotypes, no significant differences ($p > 0.05$) between genotype groups (i.e., $\varepsilon 2$ vs $\varepsilon 3$, $\varepsilon 3$ vs $\varepsilon 4$, $\varepsilon 2$ vs $\varepsilon 4$) in CBF and ATT were identified in the surface analysis. There were no significant differences ($p > 0.05$) in the extent of CBF or ATT difference with age between genotype groups nor between the means of the linear slopes of association for CBF or ATT in any cortical region (See Supplementary Material B). The rate of CBF decline was found to be significantly higher ($p_{FDR} = 0.01$) only in the right putamen for $\varepsilon 4$ carriers compared to $\varepsilon 2$ carriers.

3.4. Interactions between APOE genotype, sex, and age on perfusion measures

No significant differences in mean CBF nor ATT within sex between genotype were identified ($p > 0.05$), both for the surface analysis and slope analyses. However, Table 3 illustrates the gradients of the slope of association of perfusion measures with age on average across all 34 cortical regions between sex and *APOE* genotype. In general, female $\varepsilon 4$ individuals demonstrated the steepest slope of association with age for both CBF and ATT on average across cortical and subcortical regions, with statistical significance ($p < 0.05$). The largest significant statistical difference appeared between male $\varepsilon 2$ carriers and female $\varepsilon 4$ carriers, whereas non-statistically significant values ($p > 0.05$) were seen between female $\varepsilon 2$ carriers and female $\varepsilon 4$ carriers. The slope of association between CBF and age was generally less steep in the bilateral subcortex in comparison with the cortex. Supplementary Materials C and D demonstrates the accompanying plots of the slopes of association.

Fig. 6 shows that regions with significant differences between males and females vary according to *APOE* genotype. For ATT in $\varepsilon 4$ individuals, most sex differences were within

Author Manuscript Author Manuscript Author Manuscript Author Manuscript

the temporal cortices, whereas for $\varepsilon 2$ individuals only superior frontal regions appeared significant. For CBF in $\varepsilon 4$ individuals, sex differences were predominantly in the parietal cortex and precuneus but were located in the frontal lobe for $\varepsilon 2$ individuals. The effect size maps are independent of sample size and demonstrate distinct spatial patterns between genotypes. Supplementary Material E demonstrates the slopes of association for exemplar regions with sex differences within genotype.

To investigate this effect in more depth, we assessed the interaction of CBF and ATT for a general linear model including age, sex, cardiovascular health and *APOE* genotype as individual regressors, followed by an interaction term for only sex and *APOE* genotype in **Model 1** and an interaction term for age, sex and *APOE* genotype in **Model 2**. No significant results ($p > 0.05$) for the interaction terms were found in cortical or subcortical regions after false discovery rate correction for either model.

4. Discussion

We investigated cross-sectional associations between age, sex, *APOE* genotype and regional vascular physiology in adults with typical health. We observed reduced CBF and increased ATT with advancing age throughout much of the cerebral cortex. We also found that CBF is higher and ATT is lower overall in females compared to males independently of age and cardiovascular risk. Additionally, we investigated the potential modifying effects of sex and *APOE* genotype on age associations with perfusion measures and found unique regions affiliated with sex differences depending on *APOE* genotype. Future work modeling interaction effects in the wider consortium HCP-A sample and continuation longitudinal study may be needed to fully investigate these associations in specific regions, given the power demands of complex three-way interactions (Heo and Leon, 2010). These results underscore the potentially complex modifying effects of sex and *APOE* genotype on age-related variation in cerebral perfusion.

Effects of age on perfusion measures were present globally throughout the brain. However, there were overlapping regions where the association between CBF reduction with age and ATT increase with age were strongest. These regions included the frontal lobe and posterior cingulate cortex and were visible bilaterally. Decreases in CBF in the frontal and parietal cortices have been implicated in the aging process in previous studies (Chen et al., 2011; Wang et al., 2021). Furthermore, higher CBF in the frontal lobe has been associated better executive function and CBF reduction could be associated with frontotemporal dementias (Staffaroni et al., 2019) or small vessel disease (Markus et al., 2014). This could indicate certain regions of the cortex that are particularly vulnerable to neurodegeneration, which could be due to poor native physiology affiliated with age-related vascular changes (e.g., arterial stiffening) (Singer et al., 2014). This effect could also be linked to white matter lesion burden, which could be independently investigated as performed by van Dalen et al. (2016) to better understand local age-related microvascular changes. Our findings in the subcortex support those of Chen et al. (2011), whereby age-associated decline in CBF was less apparent in subcortical regions than in cortical regions.

Author Manuscript Author Manuscript Author Manuscript Author Manuscript

Females consistently exhibited elevated CBF and reduced ATT compared to males regardless of age. This agrees with previous findings, where Alisch et al. (2021) found elevated CBF across multiple cortical regions in females and Juttukonda et al. (2021) identified reduced ATT in females in global gray matter. One contributing factor could be the lower hematocrit identified in females, as discussed by Juttukonda and Donahue (2019), although sex hormones may also play an important role. Additionally, this effect appeared more left lateralized, supporting previous findings (Esposito et al., 1996). As reviewed extensively by Robison et al. (2019), estrogen increases cerebral blood flow and may provide neuroprotective effects; therefore, incorporating hormone levels and menopausal status into this analysis would be a crucial next step for understanding these differences.

We did not find significant differences in CBF or ATT between *APOE* genotype overall, but two key findings were observed: 1) accelerated CBF decline and ATT increase in female $\varepsilon 4$ individuals (combined heterozygotic and homozygotic carriers) on average across all cortical regions, in agreement with previous findings (Wang et al., 2021) and 2) region-specific sex differences between *APOE* genotype. Interestingly, although we found no statistically significant effects between genotype via surface and interaction analysis, the largest difference in the gradient of the slope of association for ATT incline with age and CBF decline with age was between male $\varepsilon 2$ carriers and female $\varepsilon 4$ carriers, which warrants further study in a sample-size matched cohort with higher sampling of $\varepsilon 2/\varepsilon 4$ carriers. Our findings could indicate that while females demonstrate higher CBF relative to males regardless of *APOE* status, sex is a key contributing factor as to how *APOE* genotype influences perfusion measures across the lifespan. This may support studies that suggest that sex modulates the impact of *APOE* genotype on Alzheimer's disease risk and cerebral metabolism (Altmann et al., 2014; Sampedro et al., 2015). Integration of our results with cognitive scoring and lifestyle factors in a longitudinal cohort may provide further insight into the interacting effects involved.

The findings of this study should be considered in the context of the following limitations. Firstly, despite HCP-A being one of the largest cohorts with *APOE* genotype information to date with well age-matched groups, the effects described are cross-sectional and only describe variation trends in the sample. This can be influenced by a range of factors outside of those under study; for example, HCP-A did not strictly limit caffeine intake and caffeine is known to influence CBF (Mathew and Wilson, 1985). It is unclear how this may have affected the data reported but we do not expect that this would result in any substantial bias affecting any of the specific findings reported. Equally, arterial transit artifacts remain present in multi-delay ASL which could influence the regional differences observed. As with many studies of aging of this nature, longitudinal cohorts employing multi-delay ASL methodology, given the advantages for accurate ATT quantification, will benefit the validation of our findings. Finally, females have demonstrated higher CBF in prior studies using PET (Esposito et al., 1996), which has been attributed to inherently lower hematocrit compared to males (Mahlknecht and Kaiser, 2010). However, a limitation of this study is that hematocrit was not measured for each participant. Instead, population averages were used to model hematocrit changes between sexes and across the lifespan when computing CBF, as previously described (Juttukonda et al., 2021).

Author Manuscript Author Manuscript Author Manuscript Author Manuscript

In conclusion, we have implemented an advanced perfusion imaging technique alongside novel hemodynamic modeling to better understand the physiological mechanisms of age-related variation and characterize brain health. Overall, our results confirm previous findings of age and sex-related differences in cerebral perfusion during the typical aging process while providing novel insights into the impact on arterial transit times, regional differences, and the interacting effect of *APOE* genotype on cerebral perfusion.

Supplementary Material

Refer to Web version on PubMed Central for supplementary material.

Acknowledgments

This work was supported by the National Institutes of Health/National Institute on Aging (R21AG072068, 1K01AG070318, U01AG052564, and U01AG052564-S1) and the American Heart Association (19CDA34790002). This research was made possible in part by the computational hardware generously provided by the Massachusetts Life Sciences Center (https://www.masslifesciences.com/).

Data availability

Data will be made available on request.

Abbreviations:

ATT	Arterial transit time
CBF	Cerebral blood flow
PLD	Post-labeling delay
pCASL	Pseudo-continuous arterial spin labeling
HCP-A	Human Connectome Project - Aging
MRI	Magnetic resonance imaging
FDR	False discovery rate
FWE	Family-wise error
TFCE	Threshold-free cluster enhancement

References

Alisch JS, Khattar N, Kim RW, Cortina LE, Rejimon AC, Qian W, Ferrucci L, Resnick SM, Spencer RG, Bouhrara M, 2021. Sex and age-related differences in cerebral blood flow investigated using pseudo-continuous arterial spin labeling magnetic resonance imaging. Aging (Albany NY) 13 (4), 4911. doi:10.18632/aging.202673. [PubMed: 33596183]

Altmann A, Tian L, Henderson VW, Greicius MDAlzheimer's Disease Neuroimaging Initiative Investigators, 2014. Sex modifies the APOE-related risk of developing Alzheimer disease. Ann. Neurol 75 (4), 563–573. doi:10.1002/ana.24135. [PubMed: 24623176]

Author Manuscript Author Manuscript Author Manuscript Author Manuscript

Andersson JL, Skare S, Ashburner J, 2003. How to correct susceptibility distortions in spin-echo echo-planar images: application to diffusion tensor imaging. Neuroimage 20 (2), 870–888. doi:10.1016/S1053-8119(03)00336–7. [PubMed: 14568458]

Bookheimer SY, Salat DH, Terpstra M, Ances BM, Barch DM, Buckner RL, Burgess GC, Curtiss SW, Diaz-Santos M, Elam JS, Fischl B, Greve DN, Hagy HA, Harms MP, Hatch OM, Hedden T, Hodge C, Japardi KC, Kuhn TP, …, Yacoub E, 2019. The lifespan human connectome project in aging: an overview. Neuroimage 185, 335–348. doi:10.1016/J.NEUROIMAGE.2018.10.009. [PubMed: 30332613]

Chen JJ, Rosas HD, Salat DH, 2011. Age-associated reductions in cerebral blood flow are independent from regional atrophy. Neuroimage 55 (2), 468–478. doi:10.1016/J.NEUROIMAGE.2010.12.032. [PubMed: 21167947]

Chen JJ, Rosas HD, Salat DH, 2013. The relationship between cortical blood flow and sub-cortical white-matter health across the adult age span. PLoS ONE 8 (2), e56733. doi:10.1371/JOURNAL.PONE.0056733. [PubMed: 23437228]

Cruchaga C, Kauwe JS, Mayo K, Spiegel N, Bertelsen S, Nowotny P, Shah AR, Abraham R, Hollingworth P, Harold D, Owen MM, 2010. SNPs associated with cerebrospinal fluid phospho-tau levels influence rate of decline in Alzheimer's disease. PLoS Genet 6 (9). doi:10.1371/journal.pgen.1001101, p.e1001101. [PubMed: 20862329]

Cox RW, 1996. AFNI: software for analysis and visualization of functional magnetic resonance neuroimages. Comput. Biomed. Res 29 (3), 162–173. doi:10.1006/cbmr.1996.0014. [PubMed: 8812068]

Dai W, Fong T, Jones RN, Marcantonio E, Schmitt E, Inouye SK, Alsop DC, 2017. Effects of arterial transit delay on cerebral blood flow quantification using arterial spin labeling in an elderly cohort. J. Magnet. Resonan. Imag 45 (2), 472–481. doi:10.1002/JMRI.25367.

Dale AM, Fischl B, Sereno MI, 1999. Cortical surface-based analysis: I. Segmentation and surface reconstruction. Neuroimage 9 (2), 179–194. doi:10.1006/NIMG.1998.0395. [PubMed: 9931268]

Desikan RS, Ségonne F, Fischl B, Quinn BT, Dickerson BC, Blacker D, Buckner RL, Dale AM, Maguire RP, Hyman BT, Albert MS, 2006. An automated labeling system for subdividing the human cerebral cortex on MRI scans into gyral based regions of interest. Neuroimage 31 (3), 968–980. doi:10.1016/J.NEUROIMAGE.2006.01.021. [PubMed: 16530430]

Esposito G, Van Horn JD, Weinberger DR, Berman KF, 1996. Gender differences in cerebral blood flow as a function of cognitive state with PET. J. Nucl. Med 37 (4), 559–564 [PubMed: 8691239]

Fischl B, Sereno MI, Dale AM, 1999. Cortical surface-based analysis: II: Inflation, Flattening, and a surface-based coordinate system. Neuroimage 9 (2), 195–207. doi:10.1006/NIMG.1998.0396. [PubMed: 9931269]

Fischl B, Salat DH, Busa E, Albert M, Dieterich M, Haselgrove C, Van Der Kouwe A, Killiany R, Kennedy D, Klaveness S, Montillo A, 2002. Whole brain segmentation: automated labeling of neuroanatomical structures in the human brain. Neuron 33 (3), 341–355. doi:10.1016/S0896-6273(02)00569-X. [PubMed: 11832223]

Greve DN, Salat DH, Bowen SL, Izquierdo-Garcia D, Schultz AP, Catana C, Becker JA, Svarer C, Knudsen GM, Sperling RA, Johnson KA, 2016. Different partial volume correction methods lead to different conclusions: an 18F-FDG-PET study of aging. Neuroimage 132, 334–343. doi:10.1016/J.NEUROIMAGE.2009.06.060. [PubMed: 26915497]

Greve DN, Fischl B, 2009. Accurate and robust brain image alignment using boundary-based registration. Neuroimage 48 (1), 63–72. doi:10.1016/J.NEUROIMAGE.2009.06.060. [PubMed: 19573611]

Harms MP, Somerville LH, Ances BM, Andersson J, Barch DM, Bastiani M, Bookheimer SY, Brown TB, Buckner RL, Burgess GC, Coalson TS, Chappell MA, Dapretto M, Douaud G, Fischl B, Glasser MF, Greve DN, Hodge C, Jamison KW, …, Yacoub E, 2018. Extending the human connectome project across ages: imaging protocols for the lifespan development and aging projects. Neuroimage 183, 972–984. doi:10.1016/J.NEUROIMAGE.2018.09.060. [PubMed: 30261308]

Heo M, Leon AC, 2010. Sample sizes required to detect two-way and three-way interactions involving slope differences in mixed-effects linear models. J. Biopharm. Stat 20 (4), 787–802. doi:10.1080/10543401003618819. [PubMed: 20496206]

Author Manuscript Author Manuscript Author Manuscript Author Manuscript

Juttukonda MR, Donahue MJ, 2019. Neuroimaging of vascular reserve in patients with cerebrovascular diseases. Neuroimage 187, 192–208. doi:10.1016/J.NEUROIMAGE.2017.10.015. [PubMed: 29031532]

Juttukonda MR, Li B, Almaktoum R, Stephens KA, Yochim KM, Yacoub E, Buckner RL, Salat DH, 2021. Characterizing cerebral hemodynamics across the adult lifespan with arterial spin labeling MRI data from the Human Connectome Project-Aging. Neuroimage 230. doi:10.1016/J.NEUROIMAGE.2021.117807, p.117807. [PubMed: 33524575]

Lenth RV, 2016. lsmeans: least-Squares Means version 2.30.0. R version 4.0.2, https://CRAN.R-project.org/package=lsmeans.

Li S, Wang C, Wang Z, Tan J, 2021. Involvement of cerebrovascular abnormalities in the pathogenesis and progression of Alzheimer's disease: an adrenergic approach. Aging (Albany NY) 13 (17), 21791. doi:10.18632/AGING.203482. [PubMed: 34479211]

Love S, Miners JS, 2016. Cerebrovascular disease in ageing and Alzheimer's disease. Acta Neuropathol 131 (5), 645–658. doi:10.1007/S00401-015-1522-0. [PubMed: 26711459]

Lu H, Clingman C, Golay X, van Zijl PCM, 2004. Determining the longitudinal relaxation time (T1) of blood at 3.0 Tesla. Magn. Reson. Med 52 (3), 679–682. doi:10.1002/MRM.20178. [PubMed: 15334591]

Mahlknecht U, Kaiser S, 2010. Age-related changes in peripheral blood counts in humans. Exp. Ther. Med 1 (6), 1019–1025. doi:10.3892/ETM.2010.150/HTML. [PubMed: 22993635]

Markus HS, Allan CL, Ebmeier KPPantoni L, Gorelick PB (Eds.), 2014. Cerebral Hemodynamics in Cerebral Small Vesseldisease 180–191 Eds, pp.

Mathew RJ, Wilson WH, 1985. Caffeine induced changes in cerebral circulation. Stroke 16 (5), 814–817. doi:10.1161/01.STR.16.5.814. [PubMed: 3901422]

Mokhber N, Shariatzadeh A, Avan A, Saber H, Babaei GS, Chaimowitz G and Azarpazhooh MR, 2021. Cerebral blood flow changes during aging process and in cognitive disorders: a review. Neuroradiol. J, p. 19714009211002778. 10.1177/19714009211002778

Mutsaerts HJMM, Petr J, Václavů L, van Dalen JW, Robertson AD, Caan MW, Masellis M, Nederveen AJ, Richard E, MacIntosh BJ, 2017. The spatial coefficient of variation in arterial spin labeling cerebral blood flow images. J. Cereb. Blood Flow Metabol 37 (9), 3184–3192. doi:10.1177/0271678X16683690.

OSIPI Task Force 4.1, 2022. ASL Lexicon Available online at: https://osipi.org/task-force-4-1/, (accessed January 4, 2023).

Parkes LM, Rashid W, Chard DT, Tofts PS, 2004. Normal cerebral perfusion measurements using arterial spin labeling: reproducibility, stability, and age and gender effects. Magnet. Resonan. Med.: Off. J. Int. Soc. Magnet. Resonan. Med 51 (4), 736–743. doi:10.1002/MRM.20023.

Rabinovici GD, 2019. Late-onset Alzheimer Disease. Continuum (Minneap Minn) 25, 14–33. doi:10.1212/CON.0000000000000700. [PubMed: 30707185]

Robertson T, Beveridge G, Bromley C, 2017. Allostatic load as a predictor of all-cause and cause-specific mortality in the general population: evidence from the Scottish Health Survey. PLoS ONE 12 (8), 0183297. doi:10.1371/journal.pone.0183297, p.e.

Robison LS, Gannon OJ, Salinero AE, Zuloaga KL, 2019. Contributions of sex to cerebrovascular function and pathology. Brain Res 1710, 43–60. doi:10.1016/J.BRAINRES.2018.12.030. [PubMed: 30580011]

Sampedro F, Vilaplana E, de Leon MJ, Alcolea D, Pegueroles J, Montal V, Carmona-Iragui M, Sala I, Sánchez-Saudinos MB, Antón-Aguirre S, Morenas-Rodríguez E, Camacho V, Falcón C, Pavía J, Ros D, Clarimón J, Blesa R, Lleó A, Fortea J, 2015. APOE-by-sex interactions on brain structure and metabolism in healthy elderly controls. Oncotarget 6 (29), 26663–26674. doi:10.18632/ONCOTARGET.5185. [PubMed: 26397226]

Singer J, Trollor JN, Baune BT, Sachdev PS, Smith E, 2014. Arterial stiffness, the brain and cognition: a systematic review. Ageing Res. Rev 15, 16–27. doi:10.1016/J.ARR.2014.02.002. [PubMed: 24548924]

Smith SM, Jenkinson M, Woolrich MW, Beckmann CF, Behrens TE, Johansen-Berg H, Bannister PR, De Luca M, Drobnjak I, Flitney DE, Niazy RK, 2004. Advances in functional and structural

Author Manuscript Author Manuscript Author Manuscript Author Manuscript

MR image analysis and implementation as FSL. Neuroimage 23, S208–S219. doi:10.1016/J.NEUROIMAGE.2004.07.051. [PubMed: 15501092]

Staffaroni AM, Cobigo Y, Elahi FM, Casaletto KB, Walters SM, Wolf A, Lindbergh CA, Rosen HJ, Kramer JH, 2019. A longitudinal characterization of perfusion in the aging brain and associations with cognition and neural structure. Hum. Brain Mapp 40 (12), 3522–3533. doi:10.1002/hbm.24613. [PubMed: 31062904]

van Dalen JW, Mutsaerts HJMM, Nederveen AJ, Vrenken H, Steenwijk MD, Caan MWA, Majoie CBLM, van Gool WA, Richard E, 2016. White matter hyperintensity volume and cerebral perfusion in older individuals with hypertension using arterial spin-labeling. Am. J. Neuroradiol 37 (10), 1824–1830. doi:10.3174/ajnr.A4828. [PubMed: 27282862]

Wang J, Alsop DC, Li L, Listerud J, Gonzalez-At JB, Schnall MD, Detre JA, 2002. Comparison of quantitative perfusion imaging using arterial spin labeling at 1.5 and 4.0 Tesla. Magnet. Resonan. Med.: Off. J. Int. Soc. Magnet. Resonan. Med 48 (2), 242–254. doi:10.1002/mrm.10211.

Wang DJJ, Alger JR, Qiao JX, Gunther M, Pope WB, Saver JL, Salamon N, Liebeskind DS, 2013. Multi-delay multi-parametric arterial spin-labeled perfusion MRI in acute ischemic stroke — Comparison with dynamic susceptibility contrast enhanced perfusion imaging. NeuroImage: Clin 3, 1–7. doi:10.1016/J.NICL.2013.06.017. [PubMed: 24159561]

Wang R, Oh JM, Motovylyak A, Ma Y, Sager MA, Rowley HA, Johnson KM, Gallagher CL, Carlsson CM, Bendlin BB, Johnson SC, 2021. Impact of sex and APOE ε4 on age-related cerebral perfusion trajectories in cognitively asymptomatic middle-aged and older adults: a longitudinal study. J. Cereb. Blood Flow Metabol doi:10.1177/0271678X211021313.

Wierenga CE, Clark LR, Dev SI, Shin DD, Jurick SM, Rissman RA, Liu TT, Bondi MW, 2013. Interaction of age and APOE genotype on cerebral blood flow at rest. J. Alzheimer. Dis 34 (4), 921–935. doi:10.3233/JAD-121897.

Williams DS, Detre JA, Leigh JS, Koretsky AP, 1992. Magnetic resonance imaging of perfusion using spin inversion of arterial water. Proceed. Natl. Acad. Sci 89 (1), 212–216. doi:10.1073/pnas.89.1.212.

Xu J, Moeller S, Auerbach EJ, Strupp J, Smith SM, Feinberg DA, Yacoub E, Uğurbil K, 2013. Evaluation of slice accelerations using multiband echo planar imaging at 3 T. Neuroimage 83, 991–1001. doi:10.1016/J.NEUROIMAGE.2013.07.055. [PubMed: 23899722]

Author Manuscript Author Manuscript Author Manuscript Author Manuscript

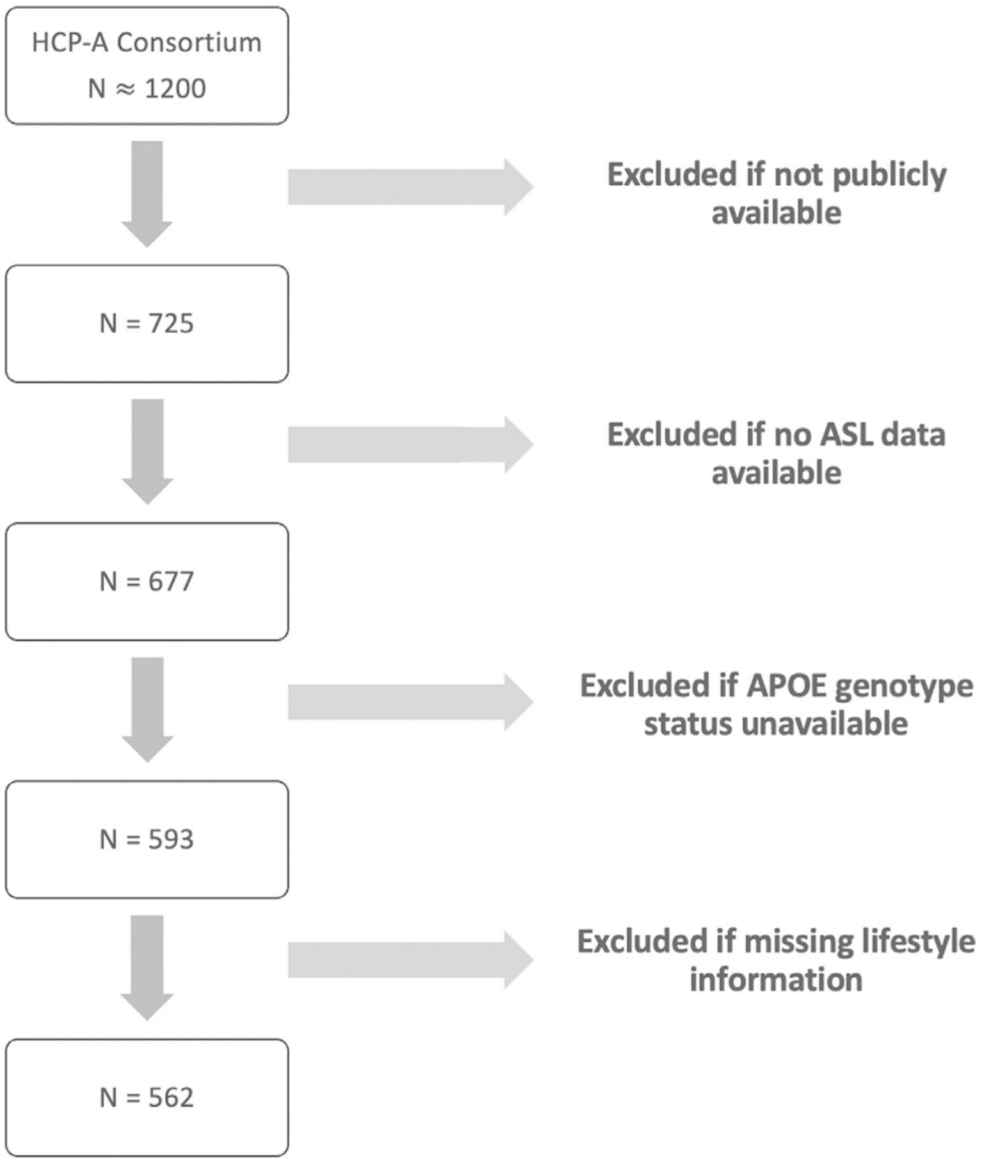

Fig. 1.
Flowchart of exclusion pipeline for participants in HCP-A cohort.

Author Manuscript
Author Manuscript
Author Manuscript
Author Manuscript

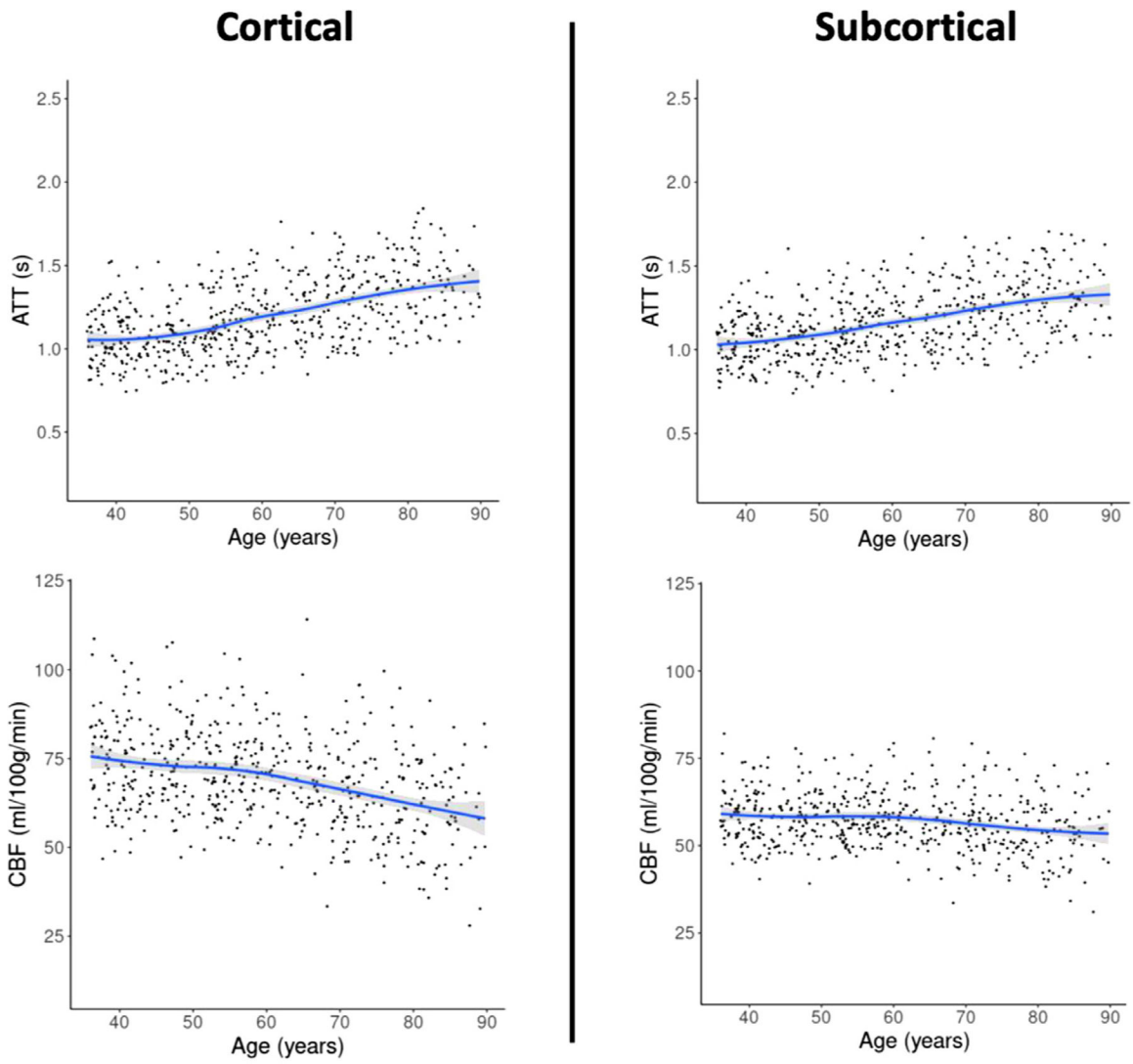

Fig. 2.

Subcortical (right) and cortical (left) CBF and ATT changes with age on average across regions and hemispheres, plotted with a non-linear slope of association. Participants over the age of 90 were removed from this visualization.

Author Manuscript Author Manuscript Author Manuscript Author Manuscript

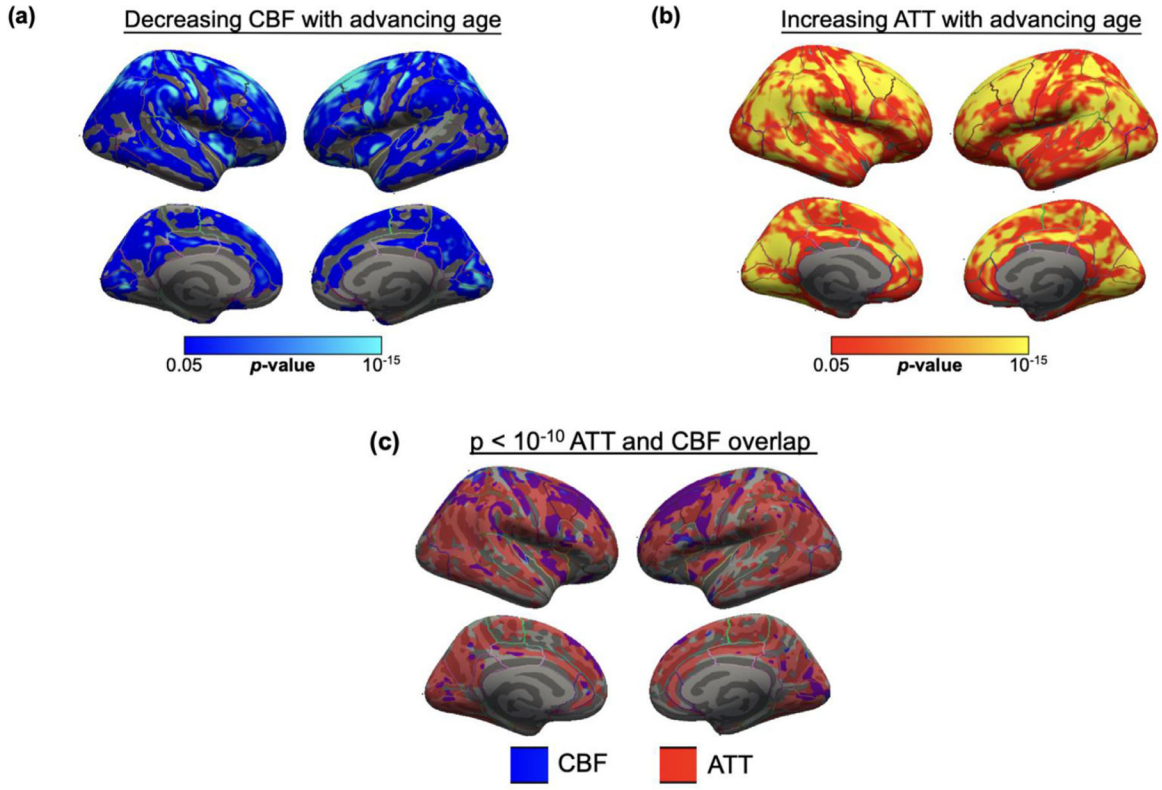

Fig. 3.

Spatial maps of surface-based group analysis for significant impact of age on (a) CBF and (b) ATT in large cohort, using Freesurfer general linear model including age as a regressor, cluster-wise corrected for multiple comparisons. Only significant statistics that survive cluster-wise correction at $p < 0.05$ are displayed. Regions with significant decline in CBF were mostly superior frontal, whereas regions with significant increase in ATT were spread across the temporal, parietal, and frontal cortices. (c) Overlap of CBF and ATT maps after thresholding at $p < 10^{-10}$, majority of overlap in the frontal and superior parietal cortices. IP = Inferior Parietal, RMF = Rostral Middle Frontal, SF = Superior Frontal, SP = Superior Parietal.

Author Manuscript Author Manuscript Author Manuscript Author Manuscript

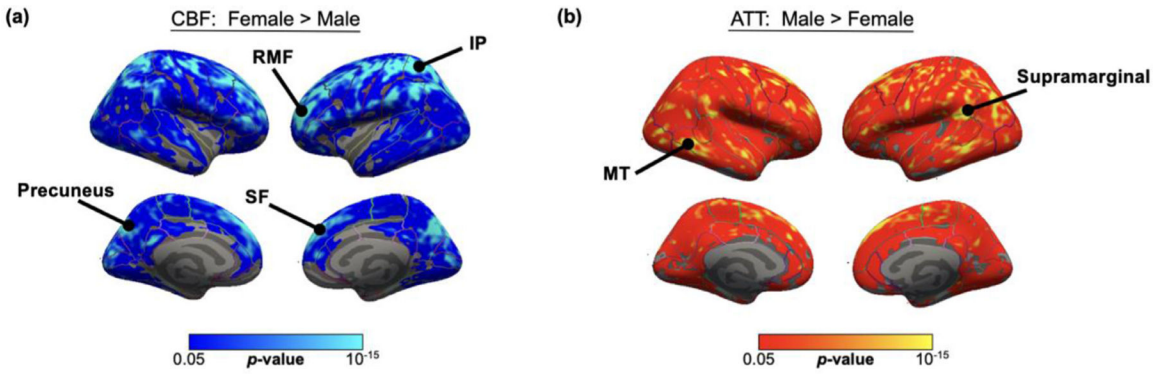

Fig. 4.

Spatial maps of surface analysis for significant impact of sex on (a) CBF and (b) ATT in large cohort, using Freesurfer general linear model including both sex and age as regressors, cluster-wise corrected for multiple comparisons. Only significant statistics that survive cluster-wise correction at $p < 0.05$ are displayed. Females demonstrated higher CBF across the parietal and frontal cortices, whereas males demonstrated higher ATT across the superior frontal cortex and temporal lobe. SF = Superior Frontal, RMF = Rostral Middle Frontal, MT = Middle Temporal, IP = Inferior Parietal, ST = Superior Temporal.

Author Manuscript Author Manuscript Author Manuscript Author Manuscript

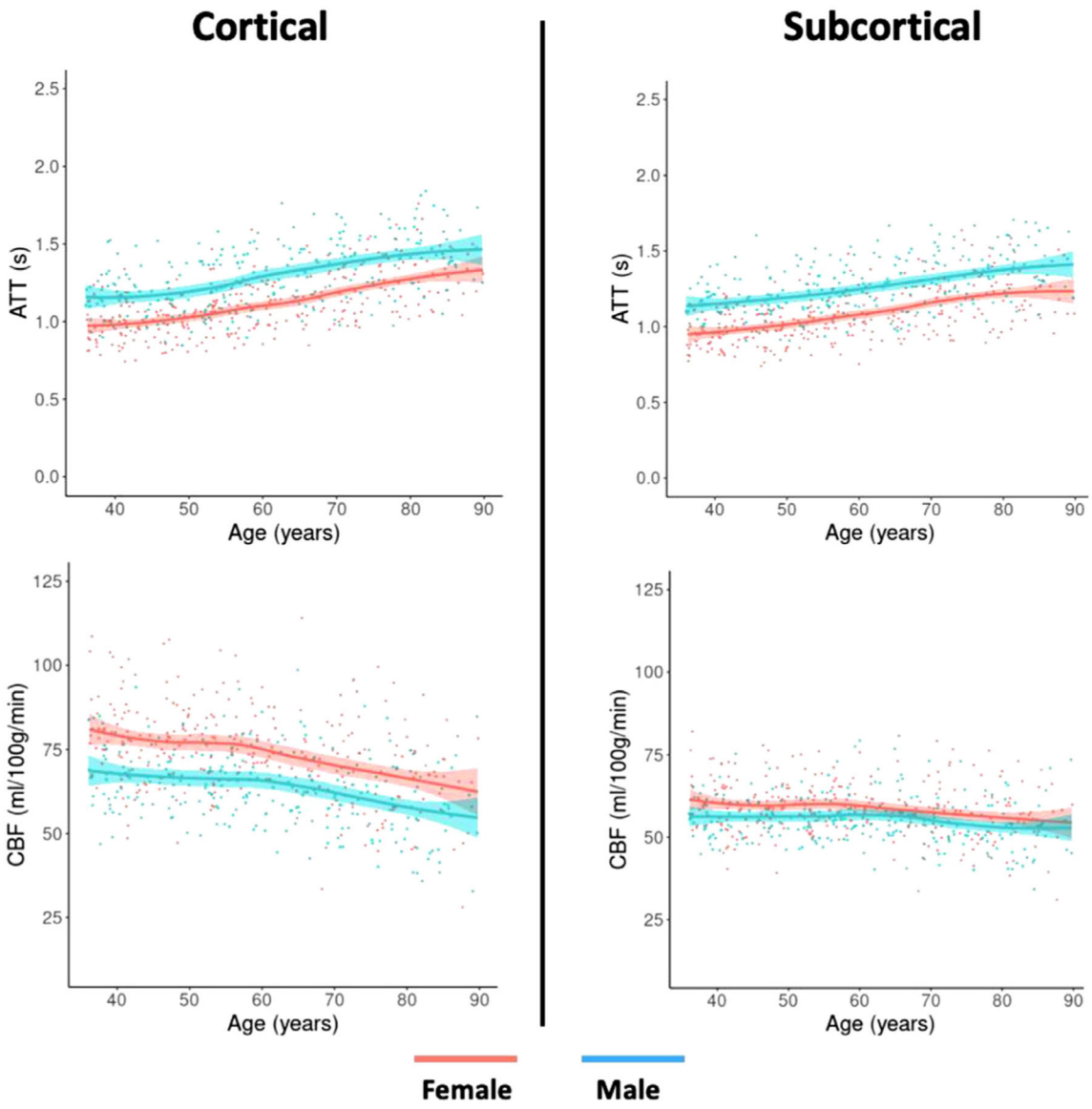

Fig. 5.

Subcortical (right) and cortical (left) CBF and ATT changes with age on average across regions and hemispheres for females (red) and males (blue), plotted with a non-linear slope of association. Participants over the age of 90 were removed from this visualization.

Author Manuscript Author Manuscript Author Manuscript Author Manuscript

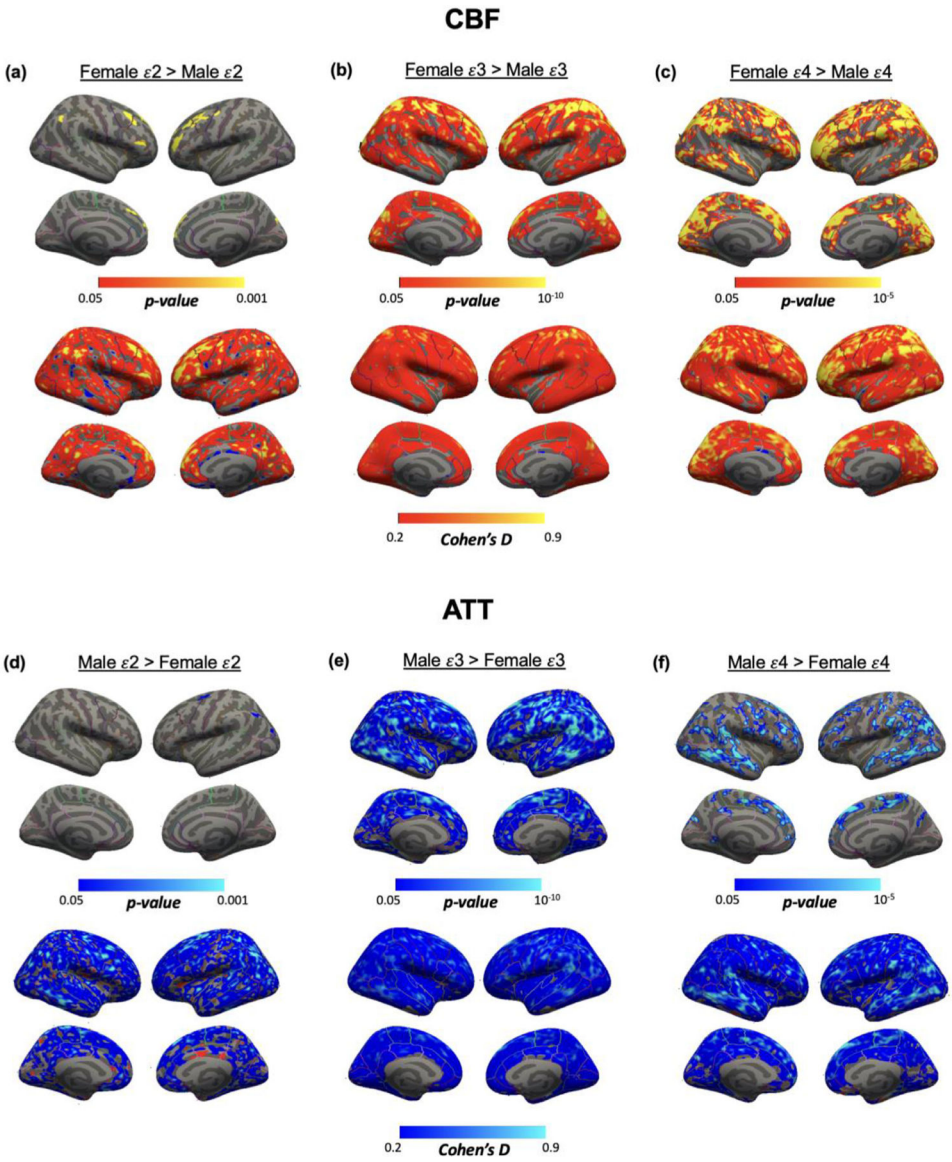

Fig. 6.

Spatial maps of surface analysis for sex differences within *APOE* genotype of (a, b, c) CBF and (d, e, f) ATT, using Freesurfer general linear model including both age and sex as regressors but only modeling the data from *APOE* genotype of interest, cluster-wise corrected for multiple comparisons. Only significant statistics that survive cluster-wise correction at $p < 0.05$ are displayed. Bottom rows show effect size maps (Cohen's D). Different spatial distributions of sex differences were identified based on *APOE* genotype.

Author Manuscript

Author Manuscript

Author Manuscript

Author Manuscript

Table 1

Demographics of interest and *APOE* stratification for the HCP-A cohort.

APOE Genotype Grouping N_{group}	**Age (years) Mean (St. Dev.)**	N_{female}/N_{total}
APOE ε3 (ε3/ε3) $N_{\varepsilon3/\varepsilon3} = 360$	60.0 (15.5)	199/360
APOE ε4 (ε2/ε4, ε4/ε4 or ε3/ε4) $N_{\varepsilon2/\varepsilon4} = 13$, $N_{\varepsilon4/\varepsilon4} = 14$, $N_{\varepsilon3/\varepsilon4} = 105$	60.8 (14.0)	70/132
APOE ε2 (ε2/ε2, ε2/ε3) $N_{\varepsilon2/\varepsilon2} = 4$, $N_{\varepsilon2/\varepsilon3} = 66$	61.7 (18.0)	38/70

Author Manuscript

Author Manuscript

Author Manuscript

Author Manuscript

Table 2

Contrasts of interest for surface-based general linear model analysis for both ATT and CBF.

Effect of age only, with cardiovascular risk regressed
Male > female, with age and cardiovascular risk regressed
$\varepsilon 2$ individuals > $\varepsilon 3$ individuals, with age and cardiovascular risk regressed
$\varepsilon 3$ individuals > $\varepsilon 4$ individuals, with age and cardiovascular risk regressed
$\varepsilon 4$ individuals > $\varepsilon 2$ individuals, with age and cardiovascular risk regressed
Female $\varepsilon 2$ individuals > male $\varepsilon 2$ individuals, with age and cardiovascular risk regressed
Female $\varepsilon 3$ individuals > male $\varepsilon 3$ individuals, with age and cardiovascular risk regressed
Female $\varepsilon 4$ individuals > male $\varepsilon 4$ individuals, with age and cardiovascular risk regressed

Author Manuscript Author Manuscript Author Manuscript Author Manuscript

Neuroimage. Author manuscript; available in PMC 2023 July 15.

Table 3

Average slope of association across regions between perfusion measures and age for each group according to hemisphere

Perfusion Measure Hemisphere	Sex and Genotype	Average Slope with Age across Brain Regions (mean +/− st. dev.)	Comparison with Female ε4 (T-statistic, p-value)
CBF		(ml/100 g/min per decade)	
Left	Female ε3	−2.90 ± 1.04	−2.94, 4.62×10^{-3} *
	Male ε3	−2.85 ± 1.05	−3.10, 2.87×10^{-3} *
	Female ε4	−3.77 ± 1.37	xxxxxxxxxxxxxxxxxx
	Male ε4	−3.19 ± 1.01	−1.99, 0.051
	Female ε2	−3.83 ± 1.68	0.14, 0.89
	Male ε2	2.41 ± 1.56	−11.26, $< 2.2\times10^{-16}$ *
Right	Female ε3	−2.78 ± 1.27	−4.67, 1.66×10^{-5} *
	Male ε3	−2.87 ± 1.15	−4.57, 2.51×10^{-5} *
	Female ε4	−4.41 ± 1.60	xxxxxxxxxxxxxxxxxx
	Male ε4	−3.35 ± 1.53	−2.81, 6.46×10^{-3} *
	Female ε2	−3.84 ± 1.70	−1.43, 0.157
	Male ε2	−0.27 ± 1.60	−10.68, 5.00×10^{-16} *
Bilateral Subcortical	Female ε3	−0.81 ± 1.01	−2.26, 0.032 *
	Male ε3	−0.90 ± 0.84	−2.19, 0.038 *
	Female ε4	−1.65 ± 0.96	xxxxxxxxxxxxxxxxxx
	Male ε4	−1.61 ± 0.88	−0.10, 0.920
	Female ε2	−1.77 ± 1.32	−0.27, 0.788
	Male ε2	0.37 ± 1.19	−4.94, 4.44×10^{-5} *
ATT		(seconds per decade)	
Left	Female ε3	0.075 ± 0.016	2.62, 0.011 *
	Male ε3	0.074 ± 0.014	3.03, 3.66×10^{-3} *
	Female ε4	0.087 ± 0.021	xxxxxxxxxxxxxxxxxx
	Male ε4	0.078 ± 0.024	1.72, 0.09
	Female ε2	0.076 ± 0.020	2.19, 0.03 *

Author Manuscript Author Manuscript Author Manuscript Author Manuscript

Perfusion Measure Hemisphere	Sex and Genotype	Average Slope with Age across Brain Regions (mean +/− st. dev.)	Comparison with Female *ε4* (T-statistic, p-value)
	Male *ε2*	0.040 ± 0.033	6.90, 5.10×10^{-9}*
Right	Female *ε3*	0.066 ± 0.015	8.11, 2.56×10^{-11}*
	Male *ε3*	0.075 ± 0.015	5.75, 2.87×10^{-7}*
	Female *ε4*	0.099 ± 0.019	xxxxxxxxxxxxxxxx
	Male *ε4*	0.083 ± 0.017	3.78, 3.38×10^{-4}*
	Female *ε2*	0.067 ± 0.013	8.09, 3.89×10^{-11}*
	Male *ε2*	0.051 ± 0.032	7.61, 4.27×10^{-10}*
Bilateral Subcortical	Female *ε3*	0.062 ± 0.011	1.65, 0.115
	Male *ε3*	0.062 ± 0.018	1.42, 0.169
	Female *ε4*	0.073 ± 0.023	xxxxxxxxxxxxxxxx
	Male *ε4*	0.055 ± 0.026	1.98, 0.058
	Female *ε2*	0.064 ± 0.020	1.19, 0.246
	Male *ε2*	0.062 ± 0.018	3.95, 6.10×10^{-4}*

* = $p < 0.05$.